

# Recloser-Fuse Coordination Recovery in Photovoltaic-Integrated Distribution Networks via Inverter Phase Angle Optimization by Quasi-Oppositional-Chaotic-Symbiotic Organisms Search Algorithm

Tuan Khanh Dang<sup>1\*</sup>, Ngoc Dieu Vo<sup>1</sup>, Hoang Khoa Truong<sup>1</sup>, Nhat Huy Huynh<sup>1</sup>,  
Ngoc Minh Nguyen<sup>2</sup>

<sup>1</sup>Ho Chi Minh City University of Technology (HCMUT), VNU-HCMC, Vietnam

<sup>2</sup>Tay Ninh Power Company, Southern Power Cooperation, Vietnam

\*Corresponding author. Email: [dtkhanh2002@hcmut.edu.vn](mailto:dtkhanh2002@hcmut.edu.vn)

## ARTICLE INFO

Received: 14/01/2025  
Revised: 31/01/2025  
Accepted: 16/06/2025  
Published: 28/11/2025

## KEYWORDS

Inverter phase angle optimization;  
Recloser-fuse coordination;  
Symbiotic Organisms Search algorithm;  
Photovoltaic systems;  
Distribution network protection.

## ABSTRACT

The paper presents the first application of the Quasi-Oppositional-Chaotic-Symbiotic Organisms Search (QOCSOS) algorithm to optimize the phase angles of inverters, aiming to minimize the discrepancy in short-circuit currents before and after integrating photovoltaic (PV) systems. This approach maintains the recloser-fuse coordination under fuse-saving schemes to address the frequent transient faults occurring in distribution networks. Depending on the location and penetration level of PV systems, recloser-fuse coordination may lose its selectivity. However, this research demonstrates that adjusting the magnitude and phase angle of inverter short-circuit currents can restore coordination without modifying the protection device settings. While the magnitude of the inverter's short-circuit current is regulated based on its characteristics, the phase angle is optimized using the QOCSOS algorithm. The effectiveness of QOCSOS in optimizing inverter phase angles is validated regardless of the PV systems' capacities and locations in the distribution network. To showcase the efficacy of the solution, the study was applied to a 22 kV distribution feeder of Tay Ninh power company, and the results were further verified through simulations in the ETAP software.

Doi: <https://doi.org/10.54644/jte.2025.1764>

Copyright © JTE. This is an open access article distributed under the terms and conditions of the [Creative Commons Attribution-NonCommercial 4.0 International License](https://creativecommons.org/licenses/by-nc/4.0/) which permits unrestricted use, distribution, and reproduction in any medium for non-commercial purpose, provided the original work is properly cited.

## 1. Introduction

Renewable energy, particularly PV systems, has significantly advanced over the past decade. As distributed energy sources, PVs connect directly to distribution grids, supplying power to loads without transmission networks. They offer benefits like reducing greenhouse gas emissions, power losses, and supporting voltage regulation and reactive power compensation. However, high PV penetration changes the magnitude and direction of short-circuit currents, challenging protection coordination, especially recloser-fuse coordination under the fuse-saving scheme.

Many solutions have been proposed to address the negative impacts of distributed energy sources on protection coordination during short-circuit events. A simple method in [1] involves disconnecting PV systems immediately upon fault detection, as required by IEEE 1574 standards [2]. However, this reduces power reliability and risks synchronization issues during reconnection [3]. Another approach in [4] limits distributed energy penetration to maintain recloser-fuse coordination, contradicting renewable energy development and environmental policies. In [5], fault current limiters (FCLs) with optimal placement and sizing are used to reduce short-circuit currents, but high costs, operational losses, and large-scale deployment challenges hinder adoption. Inverters in [6] reduce fault current output based on voltage sag, but minimizing current contributions to zero nearly disables the inverter. Studies in [7-8] adjust recloser settings or fuse sizes according to PV penetration levels, causing inconvenience due to frequent adjustments. In [9], an adaptive protection scheme uses a voltage transformer to sample measurements and restore coordination based on positive sequence impedance ratios, but the cost of voltage transformers limits practicality. Lastly, the multi-agent system (MAS) in [10] employs

intelligent electronic devices (IEDs) for optimal coordination timing, though high investment costs remain a significant barrier.

The paper proposes an effective solution by utilizing the ability to adjust both the magnitude and phase angle of inverter short-circuit currents. The magnitude is modified based on inverter characteristics, while the phase angle is optimized using the QOCSOS algorithm. This ensures the short-circuit current in PV-integrated distribution networks remains similar to that of the original network. By combining smart meter data with inverter control, the solution effectively maintains protection coordination, particularly recloser-fuse coordination, regardless of PV location or capacity.

The paper is structured as follows: Section 2 outlines the research methodology, covering the QOCSOS algorithm theory, recloser-fuse coordination based on the fuse-saving scheme, short-circuit current limitations, and inverter operational modes. It also formulates the optimization problem for inverter phase angles to minimize fault current differences caused by PV integration, restoring recloser-fuse coordination. Section 3 applies the QOCSOS algorithm to a 22 kV distribution feeder in Tay Ninh Power Company, analyzing various PV penetration scenarios, including capacity, location, and inverter phase angle control. Section 4 concludes with key findings and future research directions.

## 2. Research methodology

The paper introduces the QOCSOS algorithm and the theory of recloser-fuse coordination under the fuse-saving scheme. The algorithm optimizes inverter phase angles to minimize differences in short-circuit current magnitudes before and after PV integration. It also covers the current-limiting characteristics and operational modes of inverters. Finally, ETAP software is used to validate the results.

### 2.1. QOCSOS algorithm

The QOCSOS algorithm, an enhanced version of the SOS algorithm, integrates Quasi-Opposition-Based Learning (QOBL) and Chaotic Local Search (CLS). The process begins with a randomly initialized population of organisms, followed by the QOBL strategy to refine the initial population. It then proceeds through three stages: mutualism, commensalism, and parasitism, with QOBL applied again afterward. Finally, the CLS strategy identifies the best organism. This iterative process continues until the predefined stopping criteria are met [11]. The three stages and two strategies are detailed as follows.

#### 2.1.1. The mutualism phase

In the mutualism phase, both organisms benefit from their relationship. The vectors  $X_i$  and  $X_j$  represent the  $i$ -th and  $j$ -th organisms, which contain optimal solutions randomly selected from the initial population. Two random organisms are chosen from the population with the goal of interacting mutually and forming two new organisms,  $X_i^{new}$  and  $X_j^{new}$ , which are created according to (1) - (3). However, the new organisms are only updated if their fitness values are better than before [12].

$$X_i^{new} = X_i + \text{random}(0,1) \times (X_{best} - MV \times bf_1) \quad (1)$$

$$X_j^{new} = X_j + \text{random}(0,1) \times (X_{best} - MV \times bf_2) \quad (2)$$

$$MV = \frac{bf_1 + bf_2}{2} \quad (3)$$

Where,  $\text{rand}(0,1)$  is a vector of random numbers ranging from 0 to 1;  $X_{best}$  refers to the best organism in an ecosystem;  $MV$  is a mutual vector representing the symbiotic relationship of mutual support between organisms  $X_i$  and  $X_j$ ;  $bf_1$  and  $bf_2$  are benefit factors that describe the level of benefit for each organism, and these factors are stochastically selected as 1 or 2 (1 for partial benefit, 2 for full benefit).

#### 2.1.2. The commensalism phase

The commensalism relationship is similar to mutualism, but the difference lies in the fact that only one organism benefits, while the other neither benefits nor is harmed. In the commensalism phase, an

organism  $X_j$  is randomly selected to interact with organism  $X_i$ . A new organism,  $X_i^{new}$ , is generated through the commensal relationship with organism  $X_j$  as (4). If the fitness value of  $X_i^{new}$  is better than its previous value,  $X_i^{new}$  is updated [12].

$$X_i^{new} = X_i + random(-1,1) \times (X_{best} - X_j) \quad (4)$$

### 2.1.3. The parasitism phase

In a parasitism relationship, the parasite benefits while the host suffers adverse effects. The organism  $X_i$  is duplicated to create a *Parasite\_Vector*. Certain elements of the *Parasite\_Vector* are randomly selected and adjusted within an allowable range. Subsequently, another organism  $X_j$  from the current ecosystem is randomly selected as the host for the *Parasite\_Vector*. The fitness values of both  $X_j$  and the *Parasite\_Vector* are calculated and compared. The organism with the better fitness value is retained.

### 2.1.4. The QOBL strategy

In the QOCSOS algorithm, the QOBL strategy is applied for population initialization and generational jumps. The initialization process using QOBL generates two populations: a random population and a quasi-oppositional population. From these, a set of the best solutions is selected as the initial population. Additionally, the generational jump based on QOBL enables the algorithm to move towards a new solution with improved fitness value. The jump rate ( $jr$ ) determines whether the algorithm retains the current solution or transitions to the quasi-oppositional solution [11].

Given  $X(x_1, x_2, \dots, x_n)$  as a point in an  $n$ -dimensional space, the opposite point  $X^o(x_1^o, x_2^o, \dots, x_n^o)$  is defined by (5), while the quasi-opposite point  $X^{qo}(x_1^{qo}, x_2^{qo}, \dots, x_n^{qo})$  is defined by (6).

$$x_i^o = a_i + b_i - x_i \quad (5)$$

$$x_i^{qo} = rand\left(\frac{a_i + b_i}{2}, x_i\right) \quad (6)$$

Where,  $x_i \in \mathbb{R}, x_i \in [a_i, b_i] \forall i \in \{1, 2, \dots, n\}$

### 2.1.5. The CLS strategy

The CLS strategy is applied to the current best population in the QOCSOS algorithm to explore the search space in the vicinity of the current best solutions and generate a new solution. From the current best population, a new solution is generated according to (7) [13].

$$X_{best,k}^{new} = X_{best,k} + (Z_k - 0.5) \times (X_{i,k} - X_{j,k}) \quad (7)$$

Where,  $X_{best,k}^{new}$ ,  $X_{best,k}$  are the newly generated solution and the current best solution at the  $k$ -th iteration, respectively;  $Z_k$  is a chaotic number in the range of 0 to 1 at the  $k$ -th iteration;  $X_{i,k}$  and  $X_{j,k}$  are two solutions randomly selected from the current best population.

The chaotic coefficient  $Z_k$  is selected based on types of chaotic maps to generate random value sequences with a structured search pattern. This study uses the "logistic map" as shown in (8) [14].

$$Z_{k+1} = 4 \times Z_k \times (1 - Z_k) \quad (8)$$

Where,  $Z_0 = rand(\quad), Z_k \in (0,1) \forall k \in \{0,1,2,\dots\}$

## 2.2. The impact of PVs on recloser-fuse coordination

### 2.2.1 Recloser-fuse coordination under fuse-saving scheme

Recloser-fuse coordination under the fuse-saving scheme ensures that for transient faults, the recloser trips to protect the fuse, while for permanent faults, the fuse blows to isolate the fault. This coordination

follows conditions (9) and (10). Figure 1 (a) shows the coordination between recloser Rec\_1 and fuse Fuse\_200A.

$$I_{\min} \leq I_{Fault} \leq I_{\max} \quad (9)$$

Where,  $I_{\min}$  and  $I_{\max}$  represent the current magnitudes determined at the intersection points between the slow trip characteristic (Trip\_2) of Rec\_1 and the total cut-off curve of Fuse\_200A, and between the fast trip characteristic (Trip\_1) of Rec\_1 and the minimum melting curve of Fuse\_200A, respectively;  $I_{Fault}$  is the fault current after Fuse\_200A, as shown in Figure 1 (b).

To ensure selectivity, the minimum time gap between the minimum melting time of the fuse and the fast tripping characteristic of the recloser must be greater than 100 ms [15].

$$t_{\min\_Fuse\_200A} - t_{Rec\_1} \geq \Delta t = 100(ms) \quad (10)$$

Where,  $t_{\min\_Fuse\_200A}$  and  $t_{Rec\_1}$  represent the minimum melting time of Fuse\_200A and the tripping time of the fast trip characteristic (Trip\_1) of Rec\_1, respectively.

### 2.2.2. Four zones connecting PVs

The distribution network has four zones for PV connection, as shown in Figure 1 (b). PVs in zones I and II increase the fault current through the fuse during downstream faults, potentially violating condition (10). In contrast, zones III and IV have minimal impact on recloser-fuse coordination. This study analyzes the negative effects of PVs in zones I and II and proposes using the QOCSOS algorithm to optimize inverter phase angles to mitigate these effects.

### 2.2.3. Short-circuit current limit of the inverter

The study uses the inverter model in the ETAP software. In the short-circuit current limiting mode, the inverter is considered as a constant current source feeding into the distribution grid. The limits and parameters of the inverter are illustrated in Figure 2 (a) and Figure 2 (b). Additionally, the operational mode of the inverter in the short-circuit current limiting mode needs to be selected, including Reactive Current Priority (RCP), Real Power Priority (RPP), and User-Defined Power Factor. The first two modes do not support reducing short-circuit current during faults downstream of the fuse. However, since the phase angle of the inverters can be adjusted in the third mode, the short-circuit current from the inverters, combined with the fault current from the grid, can result in a fault current magnitude similar to that before the PV systems were integrated. These phase angles are obtained by applying the QOCSOS algorithm.

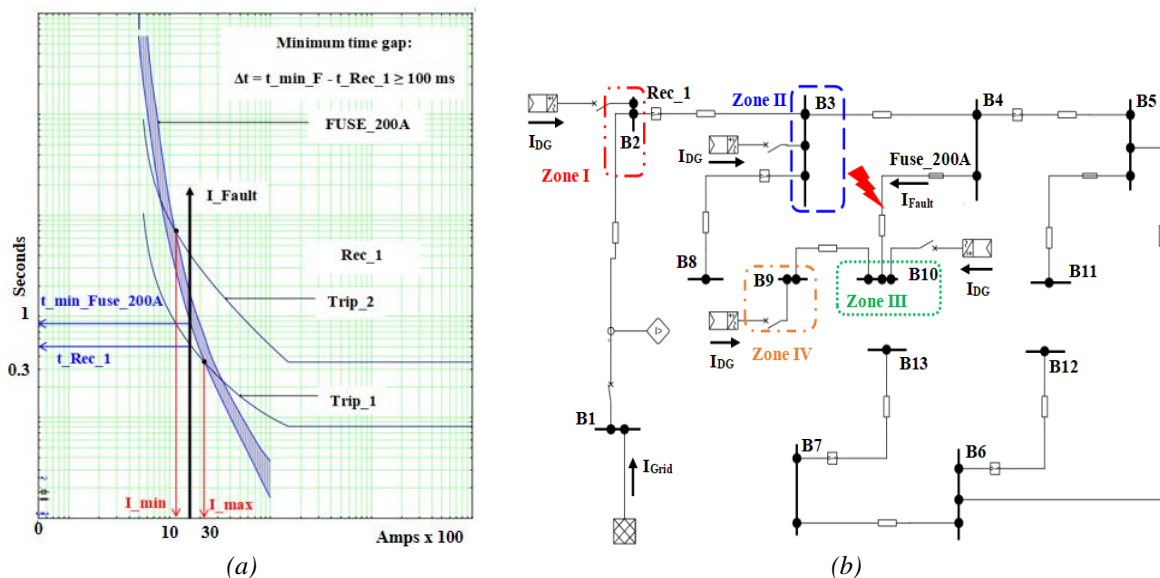
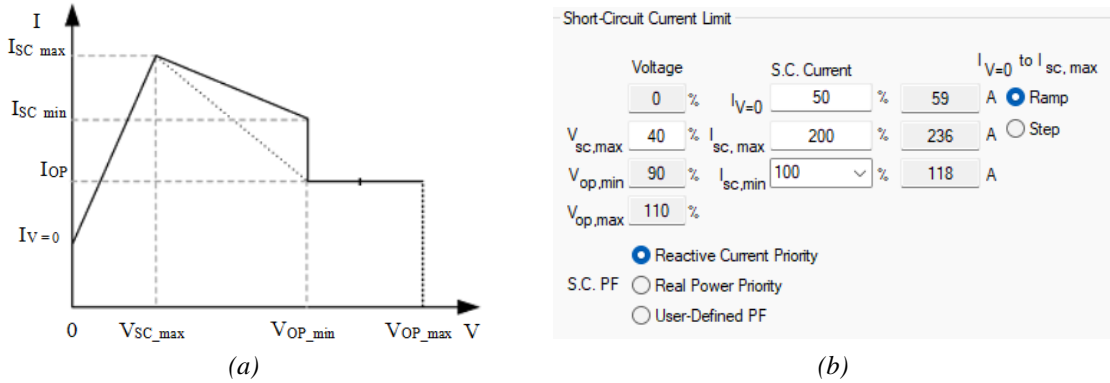


Figure 1. Recloser-fuse coordination (a): coordination principle; (b): four zones connecting PVs.



**Figure 2.** Inverter characteristic (a): short-circuit limiting curve; (b) parameters.

#### 2.2.4. Short-circuit current analysis before and after PV integration

When a short circuit occurs downstream of the fuse, it is desirable for the short-circuit current passing through the fuse and recloser to remain unchanged, regardless of whether PVs are integrated, in order to maintain the recloser-fuse coordination without violating (10). To address this issue, adjusting the phase angle of the inverter during a fault is proposed as a feasible solution based on (11).

$$\begin{cases} |\dot{I}_{Fault}^{No\_PVs}| = |\dot{I}_{Fault}^{PVs}| \\ I_{Fault}^{PVs} \angle \alpha = I_{Grid} \angle \beta + \sum_{i=1}^n (I_{PV\_i} \angle \varphi_i) \end{cases} \quad (11)$$

Where,  $(I_{Fault}^{PVs}, \alpha)$ ,  $(I_{Grid}, \beta)$ , and  $(I_{PV\_i}, \varphi_i)$  represent the magnitude and phase angle of the short-circuit current with integrated PVs flowing the fuse, the short-circuit current from the grid, and the short-circuit current from the  $i$ -th PV, respectively;  $I_{Fault}^{No\_PVs}$  denotes the magnitude of the fault current without PV integration flowing the fuse.

To perform the mathematical transformations of (11), follow the steps leading to (12) and (13).

$$\begin{cases} I_{Fault}^{PVs} \cos(\alpha) = I_{Grid} \cos(\beta) + \sum_{i=1}^n I_{PV\_i} \cos(\varphi_i) \\ I_{Fault}^{PVs} \sin(\alpha) = I_{Grid} \sin(\beta) + \sum_{i=1}^n I_{PV\_i} \sin(\varphi_i) \end{cases} \quad (12)$$

$$G(\varphi_i) = 1 - \left[ \frac{I_{Grid}}{I_{Fault}^{PVs}} \cos(\beta) + \frac{1}{I_{Fault}^{PVs}} \sum_{i=1}^n I_{PV\_i} \cos(\varphi_i) \right]^2 - \left[ \frac{I_{Grid}}{I_{Fault}^{PVs}} \sin(\beta) + \frac{1}{I_{Fault}^{PVs}} \sum_{i=1}^n I_{PV\_i} \sin(\varphi_i) \right]^2 = 0 \quad (13)$$

The phase angles of the inverters  $\varphi_i$  are the variables to be determined to satisfy (13), as the magnitudes and phase angles of the remaining currents in (13) are already defined. Indeed, the short-circuit current before the integration of PV systems  $I_{Fault}^{No\_PVs}$  is known, and the short-circuit current from the grid  $(I_{Grid}, \beta)$  is also determined. Furthermore, the magnitude of the fault current of the inverters  $I_{PV\_i}$  can be calculated based on their short-circuit current limitation characteristics, as illustrated in Fig. 2(a).

#### 2.2.5. Problem formulation

The goal is to optimize inverter phase angles to minimize the short-circuit current deviation before and after PV integration during downstream faults. The objective function is given in (14).

$$OF = \min |G(\varphi_i)| \quad (14)$$

The first constraint is that the adjustable phase angles of the inverters are limited from 0 to the maximum allowable phase angle,  $\varphi_{i\_max}$  as expressed in (15).

$$0 \leq \varphi_i \leq \varphi_{i\_max} \quad (15)$$

The second constraint is that inverters connected to the same bus, having the same terminal voltage during a fault, must be identical phase angles, as expressed in (16).

$$\begin{cases} V_j = V_i \\ \varphi_j = \varphi_i \end{cases} \quad (16)$$

The inverter phase angles from the QOCSOS algorithm are input into ETAP to verify fault current magnitudes and ensure coordination time compliance with (10).

### 2.2.6. Implementation of the QOCSOS Algorithm for Inverter Phase Angle Optimization

The initial population of the QOCSOS algorithm is a combination of a randomly initialized population and a Quasi-opposite-population, with a size of  $(NP \times D)$ . Here,  $NP$  represents the number of organisms, and  $D$  denotes the dimensionality of each organism. Each organism in this population is structured as shown in (17).

$$X_i = [\varphi_{PV\_1}, \varphi_{PV\_2}, \dots, \varphi_{PV\_n}] \quad (17)$$

The fitness of each individual is calculated using (18).

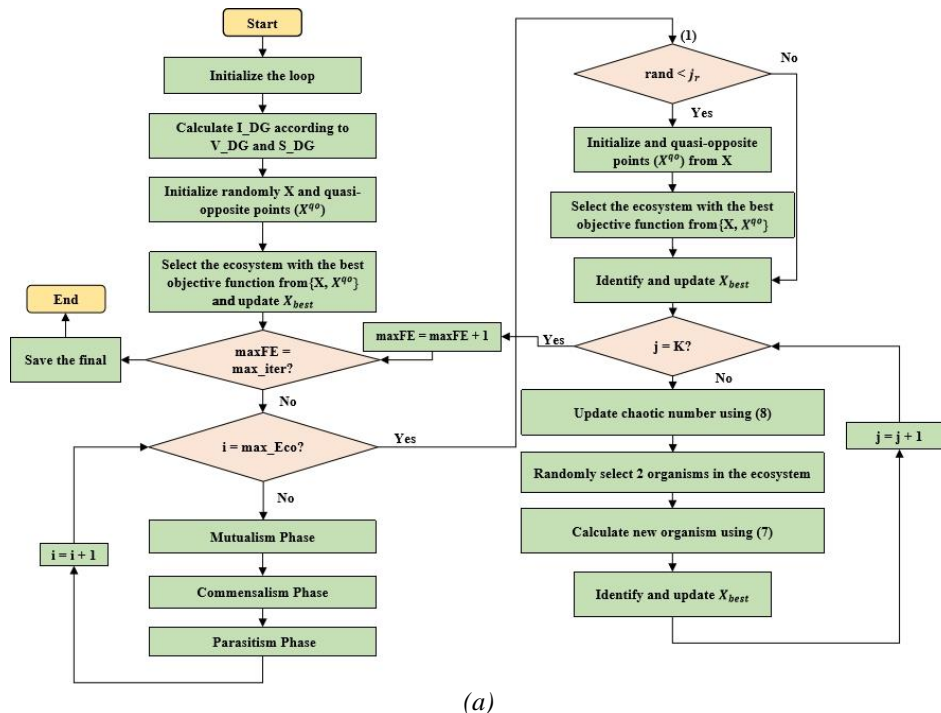
$$Fitness = OF + \alpha \sum_{Group} std(\varphi_{Group\_i}) \quad (18)$$

Where,  $OF$  is the objective function;  $\alpha$  is the penalty value for constraint violations;  $std()$  represents the standard deviation of phase angles.

The detailed calculation process is illustrated in the flowchart shown in Figure 3.

## 3. Results and discussion

### 3.1. Tay Ninh power company's 22 kV distribution feeder



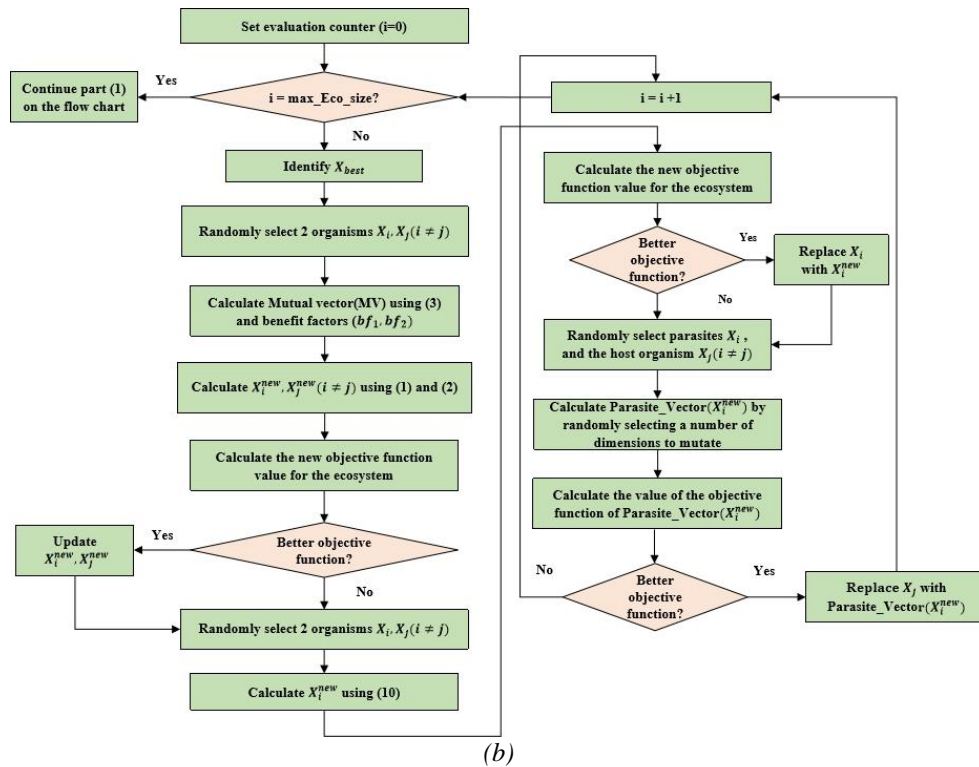


Figure 3. Algorithm flowchart (a): QOCSOS; (b) SOS.

The single-line diagram of the 22 kV distribution feeder operated by Tay Ninh Power Company is illustrated in Figure 4 (a). The key parameters of the feeder are summarized in Table 1. The coordination between Rec\_1 and Fuse\_200A is chosen as a model for detailed analysis.

### 3.2. The distribution feeder without PVs

According to the specifications of Rec\_1 and Fuse\_200A in Table 1, the simulation in ETAP software indicates that the fault current through Rec\_1 and Fuse\_200A is 1888 A, with a corresponding  $\Delta t$  of 117 ms. Since this does not violate (10), as shown in Figure 4 (b).

### 3.3. The distribution feeder with PVs

#### 3.3.1. PVs connected to only one zone

ETAP simulations (Figure 4) show that in zone I (B2), RPP mode maintains coordination ( $\Delta t > 100$  ms), while RCP mode fails from 5 MWp onwards. The QOCSOS algorithm restores coordination, achieving  $\Delta t = 117$  ms at 5 MWp with an optimal phase angle of  $8.44^\circ$  (Figure 5 (a)). In zone II (B8), RCP mode fails from 1 MWp, and RPP mode maintains coordination up to 3 MWp. The algorithm restores  $\Delta t$  to 117 ms at 9 MWp with an optimal phase angle of  $18.57^\circ$  (Figure 5 (b)).

Table 1. Key parameters of the 22 kV distribution feeder.

<b>Power grid</b>	Three-phase fault: 7.5 kA, and line-to-ground fault: 8.9 kA	<b>Fuse: Fuse_200A</b>	Type K: 200 A
<b>Total load</b>	21 MVA	<b>Cross-section of overhead line</b>	AC240, AC185, AC95, và AC70
<b>Recloser: Rec_1</b>	Pick up: 500 A, and time dial: 0.078	<b>Inverter</b>	Maximum short-circuit current is 200 % of the rate current

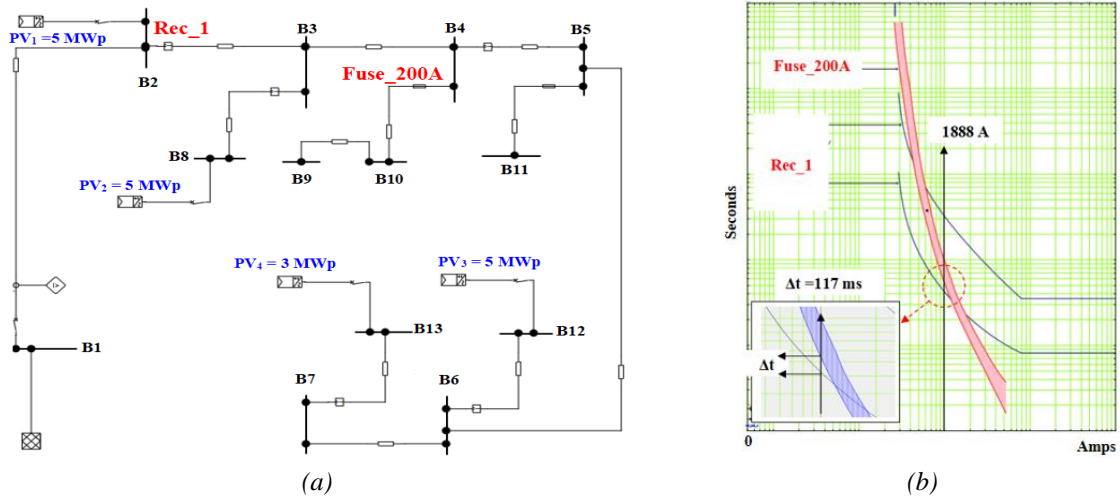


Figure 4. The 22 kV distribution feeder (a) the single-line diagram ; (b) recloser-fuse coordination .

### 3.3.2. PVs connected to multiple different zones

PVs with capacities of 5 MWp (PV<sub>1</sub>, PV<sub>2</sub>, PV<sub>3</sub>) and 3 MWp (PV<sub>4</sub>) are connected at B2, B8, B12, and B13, as shown in Figure 6 (a). ETAP simulations show that Δt is below 100 ms in both RCP and RPP modes (Figure 6 (b)). The QOCSOS algorithm is applied to restore coordination by optimizing inverter phase angles in three scenarios: (1) all inverters at the same phase angle, (2) all inverters controllable, and (3) some inverters uncontrollable. Results confirm that the algorithm restores coordination, as shown in Figures 6 (a) and 6 (b), with phase angles listed in Table 2.

Table 2. Results of phase angles for different scenarios.

<b>Scenario (1)</b>	All inverter angles are set to 17.01°	$\varphi_{PV\_i-max} = (30^0, 30^0, 30^0, 30^0)$
<b>Scenario (2)</b>	PV <sub>1</sub> : 5(29.99°), PV <sub>2</sub> : 5(18.23°), PV <sub>3</sub> :5(9.90°), PV <sub>4</sub> : 3(3.77°)	$\varphi_{PV\_i-max} = (30^0, 20^0, 10^0, 5^0)$
<b>Scenario (3)</b>	PV <sub>1</sub> : 5(29.83°), PV <sub>2</sub> : 5(19.76°), PV <sub>3</sub> :5(8.93°), PV <sub>4</sub> : 3(0°)	$\varphi_{PV\_i-max} = (30^0, 20^0, 10^0, 0^0)$

### 3.4. Discussion

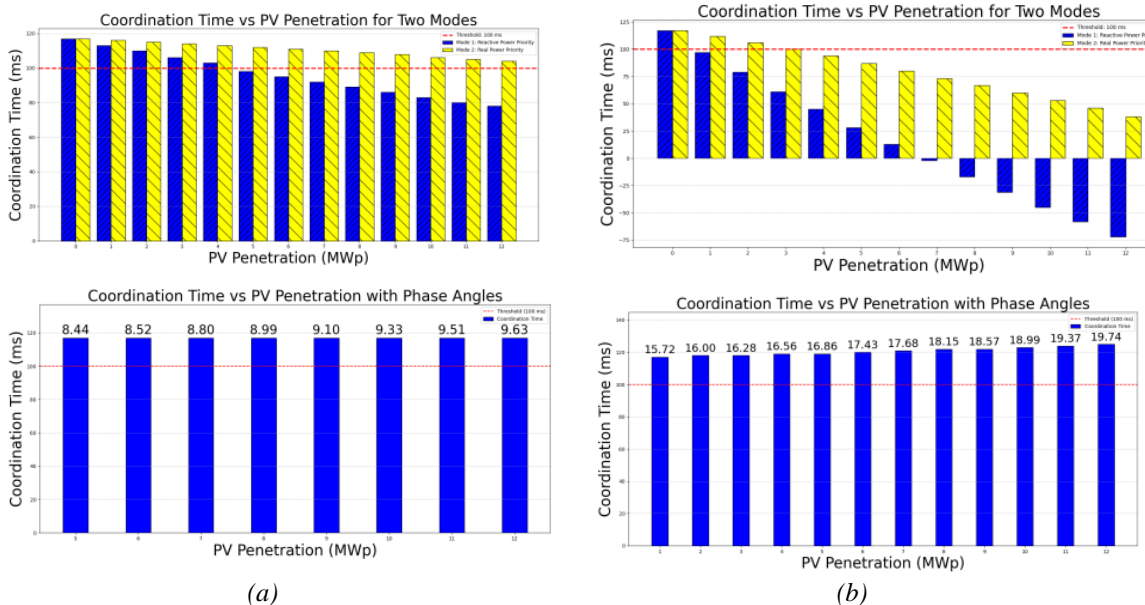


Figure 5. Δt for PVs connection to the feeder (a): zone I; (b): zone II.

Simulations indicate RCP mode adversely impacts reclosing-fuse coordination more than RPP mode, as the smaller angle between  $I_{PVi}$  and  $I_{Grid}$  leads to higher short-circuit currents and more frequent coordination violations (10). In zones I (B2) and II (B8),  $\Delta t$  in RCP mode violates coordination earlier than in RPP mode, as seen in Figure 5. The higher overload capacity of inverter semiconductor switches (2–3 times nominal value) further amplifies its impact on coordination.

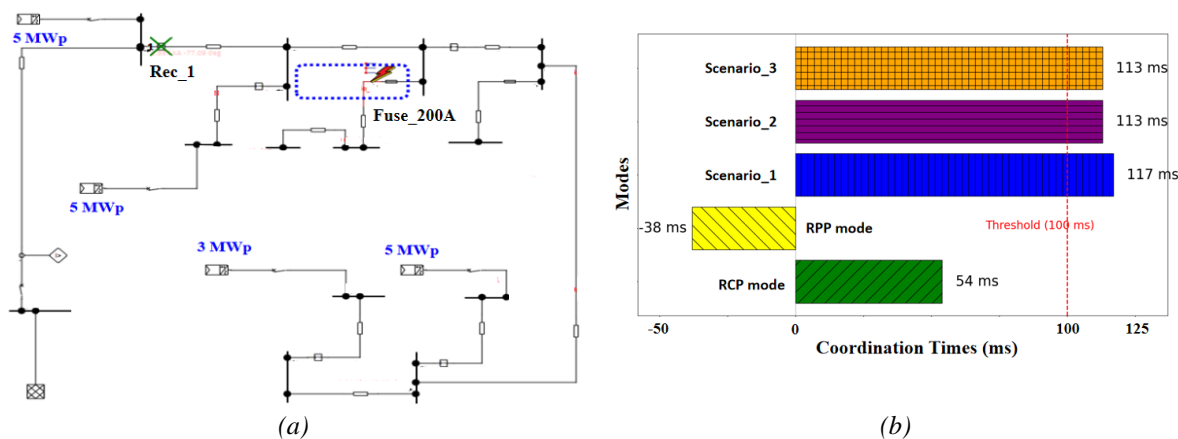


Figure 6. Simulation results (a): verification using ETAP software; (b):  $\Delta t$  for each scenario.

Table 3. Comparison of algorithm results.

Algorithms →	QOCSOS	LMDE	CMDE	GMDE
Executive time (s)	48	690	693	687
Iterations	369	20.000	20.000	20.000
Best fitness	0	0.000529	0.002980	0.000240

High PV penetration and multi-zone connections further increase coordination violations, as illustrated in Figure 6 (a), where both RCP and RPP modes fail coordination (10). This highlights the challenges posed by high PV penetration to reclosing-fuse coordination. However, adjustable inverter phase angles help mitigate short-circuit current differences and restore coordination. Regardless of whether all inverters are controllable or some are not, the QOCSOS algorithm determines optimal phase angles, as shown in Figure 6. Practically, 110 kWp inverters are typically used for PVs in distribution networks. Each 1 MWp of PV capacity requires 10 inverters, corresponding to 10 phase angle variables. With 18 MWp penetration (Section 3.3.2), there are 180 variables. To simplify operation, phase angles of PVs at the same location are constrained to be equal, facilitating management and control.

To validate the effectiveness and robustness of the algorithm, Table 3 compares convergence speed, execution time, and fitness value for scenario (2). The QOCSOS algorithm achieves the best results with an average execution time of 48 seconds, 369 iterations, and a best fitness value of 0. These results demonstrate its superiority over Modified Differential Evolution (MDE) algorithms.

#### 4. Conclusion

The paper proposes using the QOCSOS algorithm to optimize inverter phase angles, minimizing short-circuit current differences before and after PV integration, thus restoring recloser-fuse coordination under the fuse-saving scheme. These angles are determined based on pre-integration fault currents, grid fault currents, and inverter-generated fault currents. The algorithm has been successfully applied to various PV penetration scenarios in 22 kV distribution feeder of Tay Ninh power company, including capacity, location, and phase angle controllability. Detailed analyses, validated by ETAP simulations, show favorable results. Future research will expand to analyze the impact of PVs on all protective device coordination in distribution networks. For example, it could explore optimizing inverter phase angles using the QOCSOS algorithm to minimize deviations in total operating times of primary relays with or without PV integration.

## Acknowledgements

We acknowledge Ho Chi Minh City University of Technology (HCMUT), VNU-HCM for supporting this study.

## Conflict of Interest Statement

The authors declare no conflict of interest.

## REFERENCES

- [1] K. I. Jennette, C. D. Booth, F. Coffele, and A. J. Roscoe, "Investigation of the sympathetic tripping problem in power systems with large penetrations of distributed generation," *IET Gener. Transm. Distrib.*, vol. 9, no. 4, pp. 379–385, 2015.
- [2] IEEE Standard for Interconnecting Distributed Resources with Electric Power Systems, IEEE Std 1547-2003, 2003.
- [3] N. Rajaei, M. H. Ahmed, M. M. A. Salama, and R. K. Varma, "Fault current management using inverter-based distributed generators in smart grids," *IEEE Trans. Smart Grid*, vol. 5, no. 5, pp. 2183–2193, Sep. 2014. DOI: 10.1109/TSG.2014.2327167.
- [4] H. A. Abdel-Ghany, A. M. Azmy, N. I. Elkalashy, and E. M. Rashad, "Optimizing DG penetration in distribution networks concerning protection schemes and technical impact," *Electr. Power Syst. Res.*, vol. 114, pp. 113–122, 2015.
- [5] D. K. Ibrahim, E. Zahab, and A. Mostafa, "New coordination approach to minimize the number of re-adjusted relays when adding DGs in interconnected power systems with a minimum value of fault current limiter," *Electr. Power Energy Syst.*, vol. 85, pp. 32–41, 2017.
- [6] H. Yazdanpanahi, Y. Li, and W. Xu, "A new control strategy to mitigate the impact of inverter-based DGs on protection systems," *IEEE Trans. Smart Grid*, vol. 3, no. 3, pp. 1427–1436, Sep. 2012.
- [7] B. Hussain, S. M. Sharkh, and S. Hussain, "An adaptive relaying scheme for fuse saving in distribution networks with distributed generation," *IEEE Trans. Power Deliv.*, vol. 28, no. 2, pp. 669–677, 2013.
- [8] D. T. Khanh, T. H. Hoan, and T. H. B. Huy, "Optimal location and impacts of 1 MWP solar PV plants on distribution network protection," *VNUHCM J. Eng. Technol.*, vol. 4, no. 3, pp. 1036–1047, 2021.
- [9] Y. M. Makwana, B. R. Bhalja, and R. Gokaraju, "Improvement in recloser-fuse coordination technique based on modification factor," *IEEE Syst. J.*, vol. 14, no. 2, pp. 2770–2779, 2020. DOI: 10.1109/JSYST.2019.2921840.
- [10] H. Bi, B. Fani, G. Shahgholian, I. Sadeghkhani, and J. M. Guerrero, "An adaptive fuse-saving protection scheme for active distribution networks," *Int. J. Electr. Power Energy Syst.*, vol. 144, 2023.
- [11] K. H. Truong, P. Nallagownden, Z. Baharudin, and D. N. Vo, "A quasi-oppositional-chaotic symbiotic organisms search algorithm for global optimization problems," *Appl. Soft Comput.*, vol. 77, pp. 567–583, 2019.
- [12] M. Y. Cheng and D. Prayogo, "Symbiotic organisms search: A new metaheuristic optimization algorithm," *Comput. Struct.*, vol. 139, pp. 98–112, 2014.
- [13] J. Ji, S. Gao, S. Wang, Y. Tang, H. Yu, and Y. Todo, "Self-adaptive gravitational search algorithm with a modified chaotic local search," *IEEE Access*, vol. 5, pp. 17881–17895, 2017.
- [14] D. Jia, G. Zheng, and M. K. Khan, "An effective memetic differential evolution algorithm based on chaotic local search," *Inf. Sci.*, vol. 181, no. 15, pp. 3175–3187, 2011.
- [15] B. Fani, F. Hajimohammadi, M. Moazzami, and M. J. Morshed, "An adaptive current limiting strategy to prevent fuse-recloser miscoordination in PV-dominated distribution feeders," *Electr. Power Syst. Res.*, vol. 157, pp. 177–186, 2018.

**Tuan Khanh Dang** has obtained B.Eng and M.Eng. degree in Electrical Engineering from Ho Chi Minh City University of Technology (HCMUT), VNU-HCM, Vietnam in 2005 and 2008, respectively. He is currently pursuing the Ph.D at Ho Chi Minh City University of Technology (HCMUT). He is currently an senior lecturer at Ho Chi Minh City University of Technology (HCMUT), Vietnam. His research interests include power system protection, power system stability, optimization algorithms, and renewable energy.

His contact email: [dtkhanh2002@hcmut.edu.vn](mailto:dtkhanh2002@hcmut.edu.vn). ORCID: <https://orcid.org/0000-0002-0416-1050>

**Ngoc Dieu Vo** was born in Dong Thap province, Vietnam. He has received his B.Eng. and M.Eng. degrees in Electrical Engineering from Ho Chi Minh City University of Technology (HCMUT), VNU-HCM, Ho Chi Minh city, Vietnam, in 1995 and 2000, respectively, and his D.Eng. degree in Energy from Asian Institute of Technology (AIT), Pathumthani, Thailand in 2007. He is currently a lecturer at Department of Power Systems, Faculty of Electrical and Electronic Engineering, HCMUT. His interests are applications of AI in power system optimization, power system operation and control, power system analysis, and power systems under deregulation.

He can be contacted at email: [vndieu@hcmut.edu.vn](mailto:vndieu@hcmut.edu.vn). ORCID: <https://orcid.org/0000-0001-8653-5724>

**Hoang Khoa Truong** received his B.Eng. degree in Electrical Engineering from Ho Chi Minh City University of Technology (HCMUT), VNU-HCM, Vietnam, in 2012. He also received his MSc degree (Applied Sciences) and Ph.D. degree in Electrical and Electronics Engineering from Universiti Teknologi PETRONAS, Malaysia, in 2016 and 2020, respectively. He is currently a Lecturer at Department of Power Delivery, Faculty of Electrical and Electronics Engineering, Ho Chi Minh City University of Technology, VNU-HCM, Vietnam. His research interests are power system operation and control, distributed generation, microgrids, and artificial intelligence-based algorithms.

His email address is [trhkhoa@hcmut.edu.vn](mailto:trhkhoa@hcmut.edu.vn). ORCID: <https://orcid.org/0000-0002-1237-0071>

**Nhat Huy Huynh** is currently pursuing Bachelor's degree in Electrical Engineering from Ho Chi Minh City University of Technology (HCMUT), Vietnam. He has previously interned at Innovation Technology Development Corporation (INNOTECH). His research interests include power system protection, optimization algorithms, and renewable energy.

His contact email: [huy.huynhnhat11@hcmut.edu.vn](mailto:huy.huynhnhat11@hcmut.edu.vn). ORCID: <https://orcid.org/0009-0005-6623-7750>

**Ngoc Minh Nguyen** has obtained B.Eng and M.Eng. degree in Electrical Engineering from Ho Chi Minh City University of Technology (HCMUT), VNU-HCM, Vietnam in 2016 and 2024, respectively. He is currently an engineer at Tay Ninh Power Company. His research interests include power system optimization, optimization algorithms, and renewable energy.

His contact email: [nmn93tn@gmail.com](mailto:nmn93tn@gmail.com). ORCID: <https://orcid.org/0009-0004-8728-1198>